Bull. Chem. Soc. Ethiop. **2022**, 36(2), 479-485.
DOI: https://dx.doi.org/10.4314/bcse.v36i2.19

ISSN 1011-3924
Printed in Ethiopia
Online ISSN 1726-801X

STUDIES OF QUANTUM MECHANICS/MOLECULAR DOCKING ON ZANUBRUTINIB AS POTENTIAL REPURPOSED AGAINST COVID-19

Nosrat Madadi Mahani* and Sayed Zia Mohammadi

Department of Chemistry, Payame Noor University (PNU), 19395-4697, Tehran, Iran

(Received February 16, 2022; Revised April 7, 2022; Accepted April 7, 2022)

ABSTRACT. Recently, Zanubrutinib, as a novel, selective covalent and potent inhibitor Bruton's tyrosine kinase (BTK), has been used to treat COVID-19 patients. In this regard, the interaction of Zanubrutinib with Bruton's tyrosine kinase (BTK) inhibitor studied. The docking molecular and ONIOM2 (B3LYP/6-311G: UFF) methods were conducted to investigate the binding properties of Zanubrutinib with Bruton's tyrosine kinase (BTK) inhibitor. The active sites of the Bruton's tyrosine kinase (BTK) inhibitor is evaluated by docking molecular and is used for ONIOM2 calculations. The binding between Zanubrutinib and the BTK receptor is strong because values of the free binding energy are negative. The hydrogen bonds are formed between Zanubrutinib and three residues of the active amino acids Asn484, Arg 525, and Asn 526 at 2.69, 3.15, and 2.75 Å, respectively, which create through the O-atom, and the N-atom of Zanubrutinib. ONIOM2 calculation was displayed that the stability system in the solvent phase is higher than the gas-phase, which can occur due to the solvation of the species. Our results display the first mechanistic study of BTK inactivation by Zanubrutinib. This study can be helpful in the design of covalent drugs that target BTK and other similar targets.

KEY WORDS: Bruton's tyrosine kinase inhibitor, Docking molecular, Zanubrutinib, Two-layer integrated orbital molecular mechanics

INTRODUCTION

Simultaneous use of computational tools such as ONIOM (QM/MM) and molecular docking is useful to illustrate the biological ambiance which losses its nature out the live cell. Zanubrutinib is a highly selective, novel potent, and well-sustained Bruton tyrosine kinase (BTK) inhibitor [1]. Zanubrutinib is a BTK inhibitor used for the treatment of mantle cell lymphoma [2]. Also, clinical trials have illustrated that Zanubrutinib has antitumor activity in mature B-cell neoplasms [3].

The complete target blockage, increased selectivity, and longer duration of action are factors influencing the prevalence of covalent inhibitor drug discovery. Because of the function of BTK inhibitor in signal transition in the B-cell antigen receptor (BCR) pathway, inhibition of BTK is an attractive target for and autoimmune diseases and blood cancers [4, 5]. These inhibitors have also been used as possible inhibitors against the severe acute respiratory syndrome coronavirus (SARS-CoV-2) [6]. Recently, with an epidemic prevalence of Coronavirus disease (COVID)-19, the use of BTK inhibitors for treating patients has been reported that it could modify oxygenation, and reduce hypoxia and dyspnea, hypercoagulability, thrombo in flammation [7, 8].

Molecular docking can be one of the simulation methods for drug design that can be forecast the settlement of a receptor-ligand complex. The receptor is usually a nucleic acid molecule (DNA or RNA) or a protein, and the ligand could be regularly a drug [9]. Moreover, the primary method for virtual screening strategies is molecular docking.

Voice and coworkers have investigated the mechanism of covalent binding of Ibrutinib to BTK inhibitor with QM/MM computations [10]. The binding mechanism binding of human glutathione reductase enzyme and Carmustine has been studied with the DFT approach, docking molecular and dynamics simulations [11]. Ibrutinib, as a BTK Inhibitor, been investigated for the treatment of leukemia with experimental and density functional theory methods [12].

*Corresponding author. E-mail: nmmadady@gmail.com

This study is merely based on the investigation of binding affinity and the stability of Zanubrutinib with the BTK inhibitor and display interaction of the Zanubrutinib with BTK inhibitor. To distinguishing the active sites of BTK inhibitor, binding affinity, and the stability of the Zanubrutinib drug with the BTK inhibitor, superior computational methods of docking molecular and our own N-layered integrated molecular orbital and molecular mechanics (ONIOM) were used [13-16]. A molecular docking study of the Zanubrutinib molecule was performed to understand the putative binding interaction of the compound at the active site of Bruton's tyrosine kinase (BTK) as well, ONIOM2 calculation was carried out to correlate the molecular docking study and in vitro biological results.

COMPUTATIONAL DETAILS

The density functional theory (DFT) calculations are performed using the Gaussian09 program package [17] for geometry optimization and frequency computations of Zanubrutinib molecule. The B3LYP functional using 6–311G basis set [18, 19] for density functional theory calculations has been used in both gas and liquid phases.

The structure of BTK inhibitor from RCSB protein data bank and the output from DFT optimization of Zanubrutinib is obtained for molecular docking approach. To recognize the binding sites in BTK inhibitor, we performed docking calculations between Zanubrutinib as ligand and BTK inhibitor with Auto Dock 4.2 [20]. To perform molecular docking, the PDB format of the BTK inhibitor structure is built via viewer lite package.

All the water molecules have been deleted from the BTK inhibitor structure. The atoms of polar hydrogen are attached for saturation. The nonpolar hydrogen atoms are merged, and Gasteiger charges are calculated. The molecular docking was performed based on the Lamarckian genetic algorithm.

The blind docking is performed to distinguishing binding sites in the BTK inhibitor, by the grid size set to 84, 96, and 58 Angstrom along with X-, Y- and Z-axes sizes 9.526, 22.699, and -23.362 Å grid space. The best pose conformation based on the lowest inhibition constants and low inhibition constants are selected for other analyses.

The geometry optimization of a system of BTK inhibitor and Zanubrutinib was performed by an own two N-layer integrated orbital molecular mechanics (ONIOM2) approach. This method is based on dividing a molecular system into two layers that can go along by better accuracy compared and lower computational cost to the pristine DFT method [21]. The ONIOM methodology was proposed and implemented by Morokuma *et al.* [22, 23]. The ONIOM approach is a helpful method for the consideration and probing of drug delivery systems and biomolecules. By removing of the protein residues located outside the region of the active site of the receptor, the size of the system is decreased. In the ONIOM2 approach, the real molecule is divided into two parts, a small model part of the system is played at quantum mechanics (QM) level, and afterwards, the wider surrounding region has behaved at the molecular mechanics (MM) level.

QM computations on the amino acids that interact with the Zanubrutinib been carried out, and MM computations for the residual part of more extensive protein system have been performed, which is shown in Figure 1. In the BTK inhibitor, part of QM has been consisted of Asn484, Arg525, Asn 525, and Zanubrutinib (part A). While, part MM is constituted of Trp476, Gly411, Ala428, Leu408, Gln412, Val 416, Met 477, Asp 539, and Leu525, respectively (part B).

The system is optimized using the ONIOM2 approach by describing the QM region at the B3LYP/6-311G level. The MM region is treated using a universal force field (UFF). QM region has been consisted of Asn 484, Arg 525, Asn 525, and Zanubrutinib. In the ONIOM2 method, E_{ONIOM}, illustrated the total energy of the system is calculated from E^{high} of the model, E^{low} of the real and E^{low} of the model:

$$E^{ONIOM} = E^{high}(model\ system) + E^{low}(real\ system) - E^{low}(model\ system) \quad (1)$$

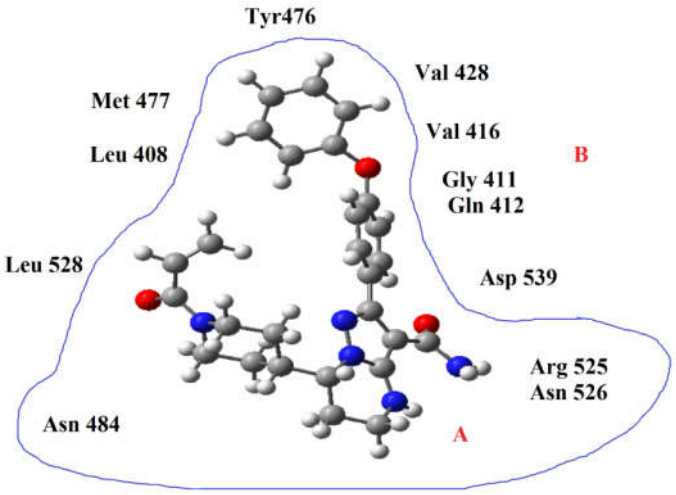

Figure 1. Schematic 2D diagram of the model system Zanubrutinib bound to BTK inhibitor binding site. Layers that are partitioned are shown for ONIOM calculations. A is the inner layer (QM: B3LYP/6-311G) and B is the outer layer (MM: UFF).

Also, the interaction energy between BTK inhibitor and Zanubrutinib, ΔE, has been obtained for specifying the stability of the system, which is given in the following formula:

$$\Delta E = \Delta E_{BTk/lig} - \Delta E_{BTK} - \Delta E_{lig} \quad (2)$$

$\Delta E_{BTK/lig}$ indicates the energy of the optimized system BTK-Zanubrutinib, ΔE_{BTK} displays the energy of the optimized BTK inhibitor, and the ΔE_{lig} is the energy of the optimized Zanubrutinib ligand. Solvent effects in interaction between Zanubrutinib drug and BTK inhibitor are investigated by the polarized continuum model (PCM) approach [24, 25].

RESULTS AND DISCUSSION

With evaluation of molecular docking calculations of Zanubrutinib–BTK inhibitor system, inhibition constant (k_I), intermolecular, internal energy, and free binding energy were obtained. The values of these parameters for the first three best-docked structures are given in Table 1.

Table 1. Docking properties for the best three docked structures. Energies are in kcal mol^{-1}.

	Free binding energy	Intermolecular energy	Internal energy	k_I (nM)
Rank: 1-1	-9.30	-11.09	-1.86	151.84
Rank: 1-2	-8.86	-10.65	-1.84	321.68
Rank: 1-3	-8.83	-10.62	-1.15	336.64

The negative value of the free the binding energy indicates which spontaneous binding occurs, and binding of Zanubrutinib with the BTK receptor is a strong binding. The best pose is obtained from Auto Dock and two dimensions structure of BTK inhibitor - Zanubrutinib is built using LigPlot [26] program and Biovia Discovery Studio [27] that is displayed in Figure 2.

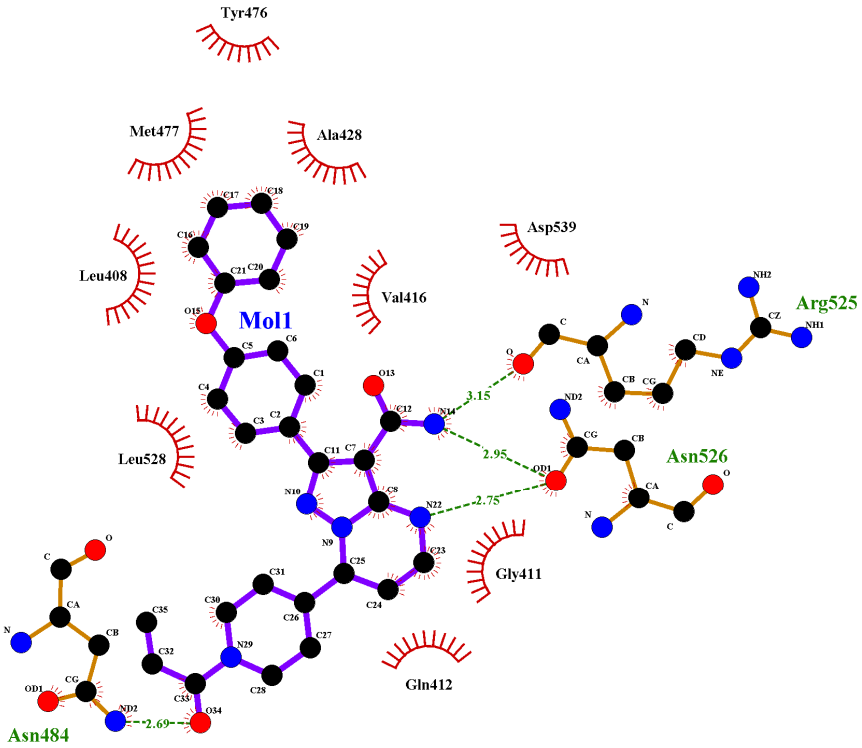

Figure 2. Binding pocket of Zanubrutinib showing the hydrophobic pocket.

The hydrophobic contacts for the ligand binding are shown in Figure 2. The hydrogen bonds are formed between Zanubrutinib, and three residues of the active amino acids Asn484, Arg525, and Asn 526 at 2.69, 3.15 and, 2.75 Å, respectively, which create through the N-atom and O-atom of Zanubrutinib.

During ONIOM2 calculations, it seems that the ligand can be formed several hydrogen bonds with the residues of the BTK inhibitor that is displayed in Figure 3. One hydrogen bonding interaction form between N-H Arg525 and O=C of Zanubrutinib at a bond distance of 2.63 Å. While, another weak hydrogen bond occurs between O=C Asn526 with N-H of Zanubrutinib. Also, A single hydrogen bonding interaction is observed between N-H Asn526 and O=C of Zanubrutinib at 2.76 Å.

The stability of the Zanubrutinib-BTK inhibitor system is investigated with the calculation of the binding energies in both the gas and the solvent phases that are listed in Table 2. Since biological interactions always do in the solvent (water) phase, so, the solvent effect in Zanubrutinib-BTK inhibitor system is performed. The binding energy in the solvent phase is higher than the gas phase that displays stability system in solvent phase increase, which can occur due to the solvation of the species.

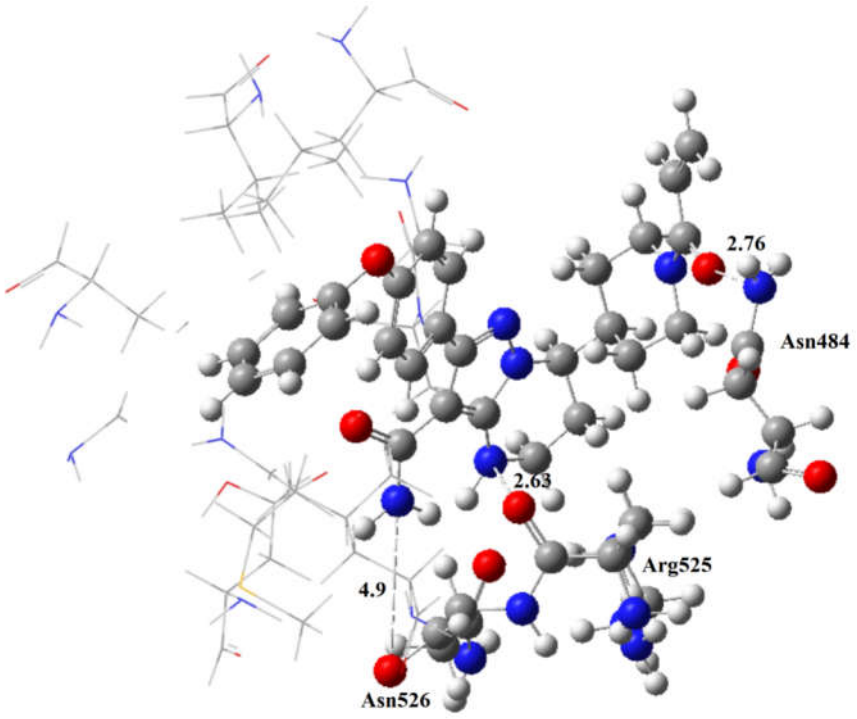

Figure 3. Optimized geometry of Zanubrutinib-BTK inhibitor system calculated at ONIOM2 (B3LYP/6-311G: UFF).

Table 2. Energy values (in au) of Zanubrutinib ligand, BTK inhibitor, Zanubrutinib-BTK inhibitor system and calculated binding energy of Zanubrutinib ligand with BTK inhibitor calculated in gas phase and solvent phase.

Phase	E_{lig}	E_{lig}/BTK	E_{BTK}	$\Delta E_{binding}$ (kcalmol^{-1})
gas	-1545.683	-2911.114	-1365.410	-0.021=-13.273
solvent	-1545.716	-2911.184	-1365.444	-0.025=-15.531

CONCLUSION

In this study, ONIOM2 (QM: MM) calculation and molecular docking are performed to look for information on Zanubrutinib ligand, BTK inhibitor and, ligand/BTK system. The active sites of BTK inhibitor are evaluated by molecular docking. The residues of Tyr 476, Val 428, Val 418, Gly411, Gln412, Asp539, Leu528, Leu408, Met477, Arg525, Asn526 and Asn434 in BTK inhibitor are active sites which Arg 525, Asn 526 and, Asn434 have essential role in binding with Zanubrutinib ligand and used in ONIOM2 computations. The ONIOM2 (QM: MM) calculations are used for the investigation of the stability and binding energies of the Zanubrutinib-BTK inhibitor system in the gas and the solvent phases. The computed binding energy in solvent phase is higher than gas phase that displays more stability of the Zanubrutinib-BTK inhibitor system in an aqueous medium.

AKNOWLEDGMENTS

We gratefully thank Payame Noor University for financial support. The authors would like to express their appreciations to department of chemistry of this university for providing research facilities.

REFERENCESS

1. Guo, Y.; Liu, Y.; Hu, N.; Yu, D.; Zhou, C.; Shi, G.; Zhang, B.; Wei, M.; Liu, J.; Luo, L.; Tang, Z.; Song, H.; Guo, Y.; Liu, X.; Su, D.; Zhang, S.; Song, X.; Zhou, X.; Hong, Y.; Chen, S. ; Cheng, Z. ; Young, S.; Wei, Q.; Wang, H.; Wang, Q.; Lv, L.; Wang, F.; Xu, H.; Sun, H.; Xing, H.; Li, N.; Zhang, W.; Wang, Z.; Liu, G.; Sun, Z.; Zhou, D.; Li, W.; Liu, L.; Wang, L.; Wang, Z. Discovery of Zanubrutinib (BGB-3111), a novel, potent, and selective covalent inhibitor of Bruton's Tyrosine Kinase. *J. Med. Chem.* **2019**, 62, 7923-7940.
2. Tam, C.S.L.; Trotman, J.; Opat, S.; Burger, J.A.; Cull, G.; Gottlieb, D.; Harrup, R.; Johnston, P.B.; Marlton, P.; Munoz, J.; Seymour, J.F.; Simpson, D.; Tedeschi, A.; Elstrom, R.; Yu, Y.; Tang ,Z.; Han, L.; Huang, J; Novotny, W.; Wang, L.; Roberts, A.W. Phase 1 study of the selective BTK inhibitor Zanubrutinib in B-cell malignancies and safety and efficacy evaluation in CLL. *Blood* **2019**, 134, 851-859.
3. Tam, C.S.; Opat, S.; Zhu, J.; Cull, G.; Gottlieb, D.; Li, J.; Marlton, P.; Qiu, L.; Roberts, A.W.; Seymour, J.F.; Simpson, D.; Song, Y.; Yang, H.; Du, C.; Feng, S.; Lin, M. Ji, L.; Novotny, W.; Wang, A.; Trotman, J. Pooled analysis of safety data from monotherapy studies of the Bruton tyrosine kinase (BTK) inhibitor, Zanubrutinib (BGB-3111) in B-cell malignancies. *HemaSphere* **2019**, 3, 526-526.
4. Pan, Z. Bruton's tyrosine kinase as a drug discovery target. *Drug News Perspect*. **2008**, 21, 357-362.
5. Zhang, Z.; Zhang, D.; Liu, Y.; Yang, D.; Ran, F.; Wang, M.L.; Zhao, G. Targeting Bruton's tyrosine kinase for the treatment of B cell associated malignancies and autoimmune diseases: Preclinical and clinical developments of small molecule inhibitors. *Arch. Pharm. Chem. Life Sci.* **2018**, 351, 1700369-1700478.
6. Roschewski, M.; Lionakis, M.S.; Sharman, J.P. ; Roswarski, J.; Goy, A.; Monticelli, M.A.; Roshon, M.; Wrzesinski, S.H.; Desai, J.V.; Zarakas, M.A.; Collen J.; Rose, K.M.; Hamdy, A.; Izumi, R.; Wright, G.W.; Chung, K.K.; Baselga, J.; Staudt, L.M.; Wilson, W.H. Inhibition of Bruton tyrosine kinase in patients with severe COVID-19. *Sci. Immunol.* **2020**, 5, 1-14.
7. Nicolson, P.L.; Welsh, J.D.; Chauhan, A.; Thomas, M.R.; Kahn, M.L.; Watson, S.P. A rationale for blocking thrombo-inflammation in COVID-19 with BTK inhibitors. *Platelets* **2020**, 31, 685-690.
8. Lin, A.Y.; Cuttica, M.J.; Ison, M.G.; Gordon, L.I. Ibrutinib for chronic lymphocytic leukemia in the setting of respiratory failure from severe COVID-19 infection: Case report and literature review. *Ejhaem* **2020**, 1, 596-600.
9. Dias, R.; de Azevedo Jr, W.F. Molecular docking algorithms. *Curr. Drug Targets* **2008**, 9, 1040-1047.
10. Voice, A.T.; Tresadern, G.; Twidale, R.M.; Vlijmen, H.V.; Mulholland, A.J. Mechanism of covalent binding of Ibrutinib to Bruton's tyrosine kinase revealed by QM/MM calculations. *Chem. Sci.* **2021**, 12, 5511-5516.
11. Begum, S.S.; Das, D.; Gour, N.K.; Chandra Deka, R. Computational modelling of nanotube delivery of anti-cancer drug into glutathione reductase enzyme. *Sci. Rep.* **2021**, 11, 4950-4964.
12. Ismail, A.I. Experimental and density functional theory characteristics of Ibrutinib, a Bruton's kinase inhibitor approved for leukemia treatment. *J. Spectros.* **2021**, 2021, 1-8.
13. Yoshida, T.; Munei, Y.; Hitaoka, S.; Chuman, H. Correlation analyses on binding affinity of substituted benzene sulfonamides with carbonic anhydrase using ab initio MO calculations on their complex structures. *J. Chem. Inf. Model.* **2010**, 50, 850-860.

14. Alzate-Morales, J.H.; Caballero, J.; Gonzalez-Nilo, F.D.; Contreras, R. A computational ONIOM model for the description of the H-bond interactions between NU2058 analogues and CDK2 active site. *Chem. Phys. Lett.* **2009**, 479, 149-155.
15. Alzate-Morales, J.H.; Caballero, J.; Jague, A.V.; Gonzalez-Nilo, F.D. Insights into the structural basis of N2 and O6 substituted guanine derivatives as cyclin-dependent kinase 2 (CDK2) inhibitors: Prediction of the binding modes and potency of the inhibitors by docking and ONIOM calculations. *J. Chem. Inf. Model.* **2009**, 49, 886-889.
16. Madadi Mahani, N. Studies on the interaction between derivatives of 9-aacridinyl amino acid as anticancer drugs and functionalized carbon nanotubes: ONIOM2-PCM approach. *Phys. Chem. Res.* **2021**, 9, 99-106.
17. Frisch, M.J.; Trucks, G.W.; Schlegel, H.B.; Scuseria, G.E.; Robb, M.A.; Cheeseman, J.R.; Montgomery Jr., J.A.; Vreven, T.; Kudin, K.N.; Burant, J.C.; Millam, J.M.; Iyengar, S.S.; Tomasi, J.; Barone, V.; Mennucci, B.; Cossi, M.; Scalmani, G.; Rega, N.; Petersson, G.A.; Nakatsuji, H.; Hada, M.; Ehara, M.; Toyota, K.; Fukuda, R.; Hasegawa, J.; Ishida, M.; Nakajima, T.; Honda, Y.; Kitao, O.; Nakai, H.; Klene, M.; Li, X.; Knox, J.E.; Ratchian, H.P.; Cross, J.B.; Adamo, C.; Jaramillo, J.; Gomperts, R.; Stratmann, R.E.; Yazyev, O.; Austin, A.J.; Cammi, R.; Pomelli, C.; Ochterski, J.W.; Ayala, P.Y.; Morokuma, K.; Voth, G.A.; Salvador, P.; Dannenberg, J.J.; Zakrzewski, V.G.; Dapprich, S.; Daniels, A.D.; Strain, M.C.; Farkas, O.; Malick, D.K.; Rabuck, A.D.; Raghavachari, K.; Foresman, J.B.; Ortiz, J.V.; Cui, Q.; Baboul, A.G.; Clifford, S.; Cioslowski, J.; Stefanov, B.B.; Liu, G.; Liashenko, A.; Piskorz, P.; Komaromi, I.; Martin, R.L.; Fox, D.J.; Keith, T.; Al-Laham, M.A.; Peng, C.Y.; Nanayakkara, A.; Challacombe, M.; Gill, P.M.W.; Johnson, B.; Chen, W.; Wong, M.W.; Gonzalez, C.; Pople, J.A. Gaussian 03, Revision A.1, Gaussian Inc.: Pittsburgh, PA; **2009**.
18. Becke, A.D. Density-functional thermochemistry. III. The role of exact exchange. *Chem. Phys.* **1993**, 58, 5648-5652.
19. Lee, C.; Yang, W.; Parr, R.G. Development of the Colle-Salvetti correlation-energy formula into a functional of the electron density. *Phys. Rev. B* **1988**, 37, 785-791.
20. Morris, G.; Huey, R. AutoDock4 and AutoDockTools4: Automated docking with selective receptor flexibility. *J. Comput. Chem.* **2009**, 30, 2785-2791.
21. Dapprich, S.; Komaromi, I.; Byun, K.S.; Morokuma, K.; Frisch, M.J. A new ONIOM implementation inGaussian98. Part I. The calculation of energies, gradients, vibrational frequencies and electric field derivatives. *J. Mol. Struct. Theochem.* **1999**, 462, 1-21.
22. Maseras, F.; Morokuma, K.IMOMM: A new integrated ab initio + molecular mechanics geometry optimization scheme of equilibrium structures and transition states. *J. Comput. Chem.* **1995**, 16, 1170-1179.
23. Morokuma, K. ONIOM and its applications to material chemistry and catalysis. *Bull. Korean Chem. Soc.* **2003**, 24, 797-801.
24. Barone, V.; Cossi, M. Quantum calculation of molecular energies and energy gradients in solution by a conductor solvent model. *J. Phys. Chem. A* **1998**, 102, 1995-2001.
25. Cossi, M.; Rega, N.; Scalmani, G.; Barone, V. Energies, structures, and electronic properties of molecules in solution with the C-PCM solvation model. *J. Comput. Chem.* **2003**, 24, 669-681.
26. Wallace, A.C.; Laskowski, R.A.; Tornton, J.M. LIGPLOT: A program to generate schematic diagrams of protein-ligand interactions. *Protein Eng.* **1996**, 8, 127-134.
27. D. Systemes, BIOVIA: Discovery Studio Visualizer, v191018287, Dassault Systèmes, San Diego; **2018**.